國防部 113 年度「補助軍事院校教師(官)從事學術研究」

研究計畫名稱:

新穎燒傷敷料之天然多聚醣結合奈米金用於大規 模戰傷缺血性傷口救護

委 託 單 位:國防部(

研 究 單 位:國防醫學院 生命科學研究所

研究計畫主持人:程君弘

協 同 研 究 人:張淑貞、范綱毅

國防部編印

中華民國 113 年 12 月 22 日

目錄

壹、摘要及成果運用	3
貳、研究動機及目的	5
参、文獻探討	6
肆、研究材料及研究方法	12
伍、研究結果	16
陸、結論與建議	23
柒、參考文獻	24

壹、摘要及成果運用

壹1. 摘要

現今國際戰爭如烏俄戰爭,凸顯了急救醫療資源並非唾手可得,在戰傷場域, 尤其即時與密集的醫療護理是重要影響士兵存活的關鍵,發經濟有效的燒傷覆 蓋敷料是燒傷治療之貢獻旨在加速傷口復原,並消除傷口感染。戰時官兵所遭 受的舉凡是複合型及大規模傷害,現有的傷口敷料通常由紗布組成,常因受限 於多處關節處無法完整包紮,也無法有效抑制細菌的生長,甚至控制傷口癒合 狀況。因應臺灣為一海島,戰爭時期容易被包圍切斷資源供給,但是海洋資源 豐沛與紡織工業技術發達,所以利用現有海洋資源以紡織技術加工的戰傷敷料 成為一個可行方向。嚴重燒傷傷口常因傷口局部血液循環不良、缺乏氧氣供應 而導致傷口修復困難,導致患者需要密切的傷口護理,並消耗大量醫療人力及 資源,因此如何改善慢性傷口的修復是醫療所需面對的重大課題。根據團隊過 去研究經驗,藻酸鹽(Alginate) 會吸收傷口滲出液形成凝膠基質,且能藉由摻 入具有抑菌特性的生物活性物質,例如金屬離子、微量元素等,來改變或強化 原有特性,加速癒合過程。奈米金 (gold nanoparticles, AuNPs) 不會被代謝降解 而存留於組織中,藉由奈米金的抗氧化特性可以進一步誘導免疫細胞的活化。 在本計畫中,我們使用氣化亞鈷 (CoCl₂) 刺激人類臍靜脈內皮細胞 (Human Umbilical Vein Endothelial Cell, HUVEC),模擬慢性傷口細胞缺氧環境,並藉由 檢測細胞存活度、基因表現,探討奈米金嫁接藻酸鈣鹽 (AuNPs-Alginate) 在協 助慢性傷口修復方面的機制。實驗結果顯示,AuNPs-Alginate 能藉由其優異的 抗氧化作用來調節慢性傷口的缺氧狀態,加速修復過程,具備成為新穎有效傷 口敷料之潛力。

壹2.成果運用

目前的實驗結果可以幫助我們了解 AuNPs-Alginate 複合物如何藉由其抗氧化作用來緩解慢性傷口氧化壓力,促使傷口癒合;而細胞組織損傷、缺氧、發炎均會導致氧化壓力上升,未來可再增加檢測發炎相關生物標記以獲得更完整的實驗數據,協助未來開發 AuNPs-Alginate 創新傷口敷料。

壹3.關鍵詞

關鍵字: 藻酸鈣鹽、奈米金、抗氧化能力、慢性傷口修復

Key word: Alginate, gold nanoparticles, antioxidant capacity, wound healing

壹4.本研究對國防之貢獻

在軍陣醫學中燒燙傷之研究是一個重要的課題,日常和戰爭的燒傷創傷處理有許多相似之處,然而,在戰區環境中,軍事燒傷具有獨特的挑戰,這使得處理起來更加困難。戰場上當燒燙傷發生後往往需要比日常多好幾倍的時間才能夠後送進入醫院治診療手術,因此戰傷治療需要一整條的行動鏈,從鄰兵戰友提供的緊急救護開始,再到後續手術室的手術措施。考量到戰場高動能武器所帶來的高溫燒灼複雜性傷口常伴隨感染、發炎,需較長的癒合時間,因此若有燒灼傷癒合加速且具傷口環境調控功能的第一線燒傷照護衛材出現,將可大大提升傷患復原的狀況,加速國軍官兵返回崗位增加前線單位之續戰量能。透過這項研究能夠幫助我們了解 Alginate 和 AuNPs 如何通過減少氧化壓力和調節細胞因子來影響傷口癒合。藉由本計畫所發展出的生物相容性材料,不僅能於動物實驗中達到顯著皮膚組織修復效果,也能進入應用於人體臨床之修復策略,提供臨床更直接及可行之治療策略思維。如能成功開發此治療方式,將可提升整體醫療能力並降低研發所需之成本。

貳、研究動機及目的

由於天然多醣可以調節燒傷微環境中的炎症反應,通過對炎性細胞因子的分析,發現天然多醣分子對細胞複製、凋亡訊息傳導的影響。若天然多醣Alginate 具有顯著調控細胞複製、凋亡及傷口免疫反應來幫助燙傷傷口組織修復之正面效果,未來也可評估用於臨床燙傷病人治療,這將會是燒燙傷病人的一大福音,亦有可能成為燒燙傷治療照護的新策略。根據團隊過去研究經驗藻酸鹽鈣具有吸收傷口滲出液形成凝膠基質的優點,適合傷口照護換藥之便利,此外團隊利用奈米金(AuNPs)強催化能力,可以將加速藻酸鹽鈣的鈣/鈉離子交換速度,加速傷口組織滲液的析出、控制發炎及促進上皮修復,因此本案結合奈米金(AuNPs)的天然多醣藻酸鹽 Alginate 之綜合應用材料 AuNPs-Alginate,分別測試在人臍靜脈內皮細胞(HUVEC)之血管損傷修復體外實驗模型以及燒傷大鼠傷口修復之體內實驗模型,評估傷口修復效益。

本研究將進行

- 一、利用天然多聚醣生物相容材料結合奈米金複合物(AuNPs-Alginate)製成 燒傷傷口治療劑。
- 二、AuNPs-Alginate 進行生物相容性試驗以確定是否適合 HUVEC 細胞複製與抗氧化效果。
- 三、測試 AuNPs-Alginate 包覆大鼠燙傷傷口,於大鼠模式中確認天然多聚醣生物相容材料可否提供損傷區域結構蛋白來降低疤痕結締組織之形成,及促使損傷區域之皮膚再生效果。

參、文獻探討

1. Wound healing progress

The skin is the organ with the largest surface area in the human body, and it is a critical structure for protecting internal tissues from mechanical damage, microbial infections, UV radiation, and extreme temperatures. It is prone to injury and has significant implications for both patients and healthcare. In the United States alone, treating non-healing wounds costs about \$50 billion, treating surgical incisions and wounds accounts for \$12 billion, and treating burns costs \$1 billion in annual health care costs [1,2]. Diabetic patients or the elderly are particularly prone to problems with wound healing, leading to long-term sequelae. However, the current treatment measures have not been significantly effective, and more effective wound healing methods are currently needed.

Most biological processes go through certain steps or stages, eg, protein synthesis, wound repair, fracture healing, and there are signal sequences that coordinate these stages. When these steps are dysregulated, associated pathologies, eg, tortuosity of blood vessels, disorganized tissue arrangement, and leakage of tissue fluid, occur; this is due to its excess of vascular endothelial growth factor (VEGF) [3]. The vessel growth step is to deliver VEGF protein first, followed by delayed delivery of platelet-derived growth factor (PDGF) to make the structure more mature and stable [4,5]. Another is the long-term inflammatory response observed in chronic wounds. The normal wound healing process begins with the production of pro-inflammatory "M1" polarized macrophages, followed by the repair of "M2" polarized macrophages [6,7]; this normal process does not occur in chronic wounds. Wound healing is sequential: (1) hemostasis - blood coagulation; (2) inflammatory response - cells fight infection and clear debris; (3) granulation - fibroblasts from the immature matrix and initiate epidermal regeneration and angiogenesis; (4) Remodeling -the new tissue is aligned correctly [8]. The progress of wound healing as Figures I below.

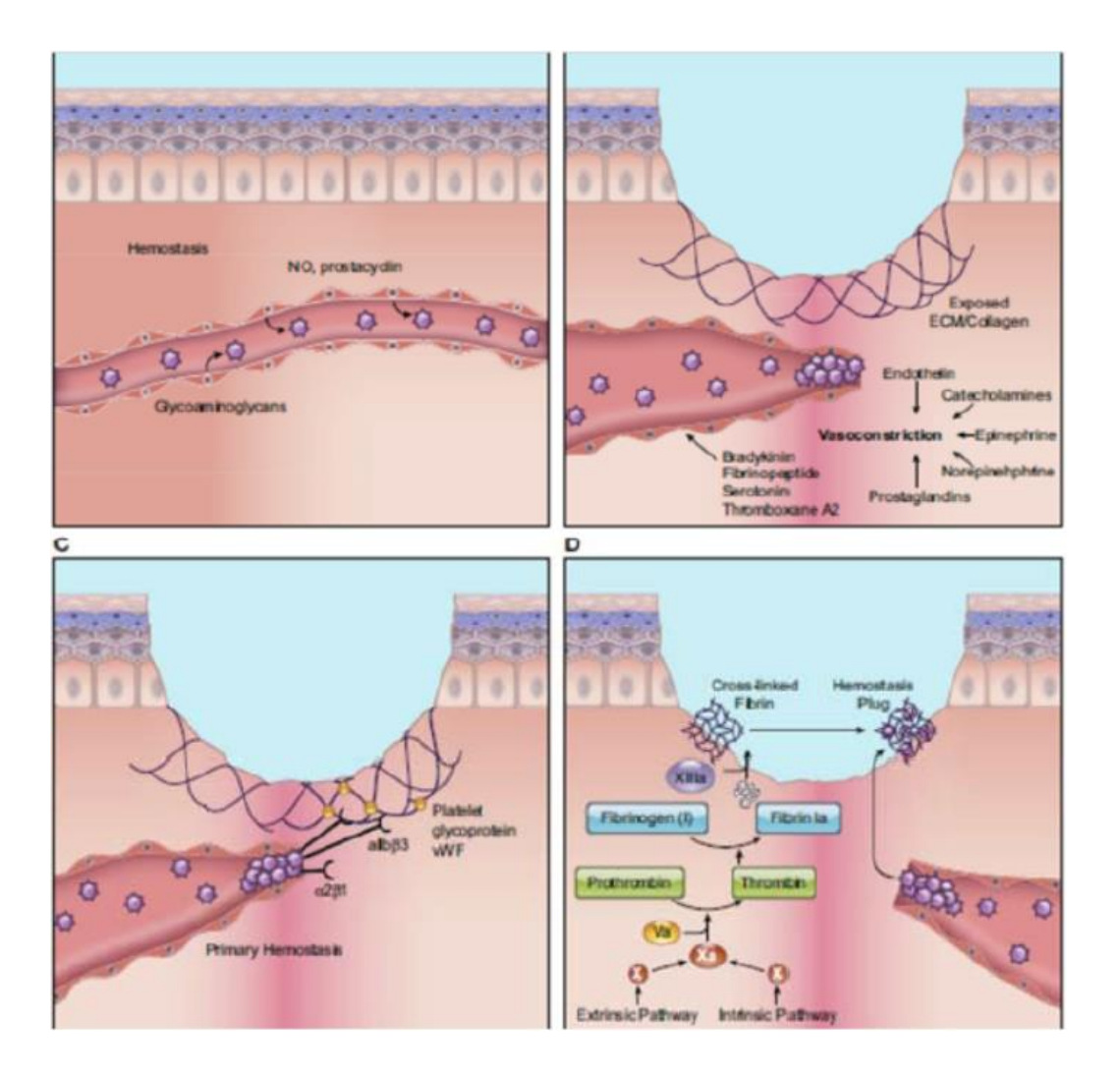


Figure I. Cellular responses during the hemostasis phase of wound healing. A: during hemostasis, platelets circulate in close proximity to the vessel wall. However, anti-thrombotic agents such as nitric oxide (NO) and prostacyclin released from endothelial cells prevent platelet attachment to the endothelial lining and platelet aggregation. B: wounding stimulates injured cells to rapidly release vasoconstrictors that cause reflexive contracture of the smooth muscle and temporary stoppage of bleeding. C: blood vessel rupture during wound healing exposes the subendothelial matrix. Platelets bind this subendothelial matrix and to each other using G proteincoupled receptors, integrins, and glycoproteins on their surface. von Willebrand factor (vWF) released by platelets also attaches to the subendothelial matrix. Platelets bind extracellular vWF through their surface receptors, strengthening the platelet plug. D: the extrinsic and intrinsic pathways lead to the activation of Factor X, which ultimately results in the cleavage of fibrinogen to fibrin. Cross-linked fibrin binds the aggregated platelet plug to form the thrombus that stops blood flow and provides a provisional matrix for healing. The illustration is a simplified rendering based on current knowledge [9].

Wound healing involves several steps, so it is important to understand the first signals of activated cellular responses in injured tissue. Wounds first initiate pathways that are easily activated. Includes Ca²⁺ waves, reactive oxygen species (ROS), and purified molecules. Increased intracellular Ca2+ appears in the first few minutes of wound edge injury and spreads to the center of the wound [10]. Damage-Associated Molecular Patterns (DAMPs), hydrogen peroxide (H2O2), lipid mediators, and signals released by damaged cells with chemokines also recruit inflammatory cells, especially neutrophils. DAMP molecules include DNA, peptides, ECM components, ATP, and uric acid, among others. The research of the organism has proved that H2O2 is rapidly produced in the wound to reduce the occurrence of infection, activate the regeneration of keratinocytes, recruit neutrophils, and promote the formation of new blood vessels [11] as Figure II below.

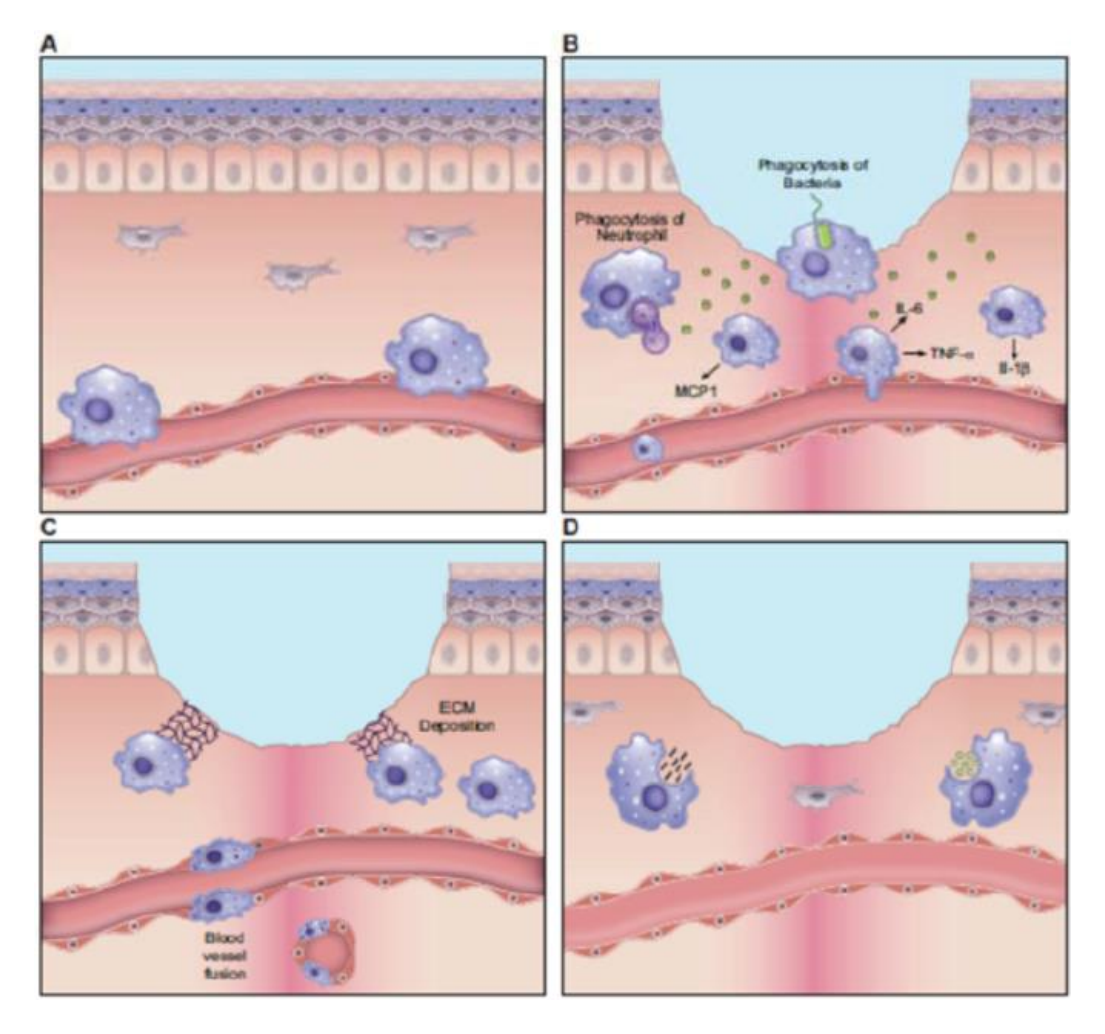


Figure II. Macrophage phenotypes in wound healing. A: in the uninjured skin, circulating monocytes from the bone marrow are constantly rolling over the inner endothelial wall within the vessel lumen and surveying for damage. The few macrophages that are resident in the skin are prevalent in the perivascular space and

can be from embryonic sources. B: following skin injury, during the inflammatory phase of healing, macrophages release pro-inflammatory cytokines such as interleukin (IL)-6, tumor necrosis factor (TNF)-α, and IL-1 to fight infection. Early macrophages in the wound release monocyte chemoattractant protein (MCP)-1 to draw in more monocytes from the bone marrow and heighten the macrophage response. These macrophages also actively participate in phagocytosis of pathogens. At the end of the inflammatory phase, macrophages engulf dying neutrophils, which marks the end of the inflammatory phase of wound healing. C: during the growth stage of wound healing, as granulation tissue forms, macrophages release growth factors such as vascular endothelial growth factor (VEGF) and platelet-derived growth factor (PDGF) that are used to signal and activate endothelial cells to perform angiogenesis. Some macrophages deposit extracellular matrix (ECM) at this stage. Unregulated deposition of ECM can lead to fibrosis, and such scar-forming macrophages are called fibrocytes. D: during wound remodeling, macrophages again take on a phagocytic role where they engulf both cell debris and excessive ECM, to bring the healed skin to a homeostatic state. The illustration is a simplified rendering based on current knowledge [9].

2. The composition of calcium alginate (CA) and its application on wound healing

Marine-derived polysaccharide, such as alginates, refined from brown seaweeds, is a natural fiber. Its chemical formula is (C6H8O6) n (Figure III), with a molar mass ranging from 10,000 to 600,000. It usually comes in white to yellowish filamentous, granular, or powdered forms. Alginates can form hydrogels with cations, namely, sodium alginate, commercially known as alginate gel, fucoidan. Alginate is mainly used as an ingredient for skin wound dressings in wound healing. These dressings are usually composed of calcium alginate or sodium alginate. When produced into dressings, alginate gels are useful in promoting healing as they are capable of absorbing wound exudate and therefore can reduce wound infiltration and avoid bacterial infection [12]. The gelling properties of alginates are the reaction between calcium wound exudate and blood, forming a colloid-polymer mixture that achieves protection [13]. Many research findings suggest that alginate dressings can enhance fibroblast proliferation and activate macrophages to produce tumor necrosis factor protein that leads to inflammation, thereby promoting wound healing. The release of calcium from the dressings into the wounds can also create agglutination that promotes homeostasis [14]. This kind of dressing fiber can accelerate degradation and can also be cleaned with saline water, reducing the pain while replacing the dressing to avoid destruction of granulation tissue [15].

Figure III The chemical structure of alginates compound.

Alginate polymers are widely used in food and medicine. Alginate dressing is a kind of wound with good biocompatibility [16]. CA is an ideal filler that is easy to fold and apply to wound healing [17]. In addition, the water absorption capacity is very good. It can absorb 20 times its volume of water and 5 to 7 times that of traditional gauze [18]. In addition, calcium alginate dressings can exchange calcium ions when applied to wounds, helping to stop bleeding [19,20]. Therefore, it can be used as a postoperative wound dressing During wound healing process, tissue exudate stuck to dressing, pulling during dressing change caused secondary trauma, increased pain sensation of patients, delayed healing produced scar tissue, and caused difficulty in wound management. Therefore, it was urgently needed to develop dressing that could not cause adhesion. George Blaine extracted Sodium alginate (SA) from seaweed in 1947. It is a kind of polysaccharide Glycosaminoglycans (GAGs) protein that is made of Calcium ion coagulant and processed into gauze-type non-woven fabric by wet spinning. Due to good water retention, nonadherent Hydrogel will be formed after water absorption to reduce wound adhesion and maintain wound healing in a moist environment to accelerate. Current researches of the SA to participate in the regulation of inflammation, Masahito et al. Study of SA can alleviate mice induced by diethylnitrosamine nonalcoholic fatty hepatitis, liver tissue inflammation index TNF-α, IL-6, F4/80, the CCL2 and peroxide channel signal in serum were significantly lower, CA can improve long-term inflammation and oxidative stress [21].

3. Gold nanoparticles (AuNPs) applications

The use of metallic nanoparticles (NPs) has greatly expanded in many biomedical fields nowadays due to their similarity to the nanostructured nature of the microenvironment. Not only do NP's possess a unique set of properties, including

small size and large surface area to volume ratios, but they are also able to activate molecular signaling pathways [22]. Additionally, previous studies have revealed the applications of the NPs in wound dressings to help protect against infection make these NPs highly useful in wound care [22,23]. AuNPs have intrinsic antibacterial and antioxidant properties that promote the healing process through hemostasis and inflammatory phases [24]. Further research has shown AuNPs as promising bactericidal agents due to their versatile optical and photothermal properties [25]. Moreover, AuNPs as topical treatment ingredients has been shown to be capable of penetrating the skin barrier and affecting epidermal cells. A previous study also demonstrated that using AuNPs combined with antioxidant drugs displayed an acceleration in wound healing, correlating with modulation of inflammation and angiogenesis in mice wound injury model [26]. When an antioxidant phytochemical decoration is coated on AuNPs, cutaneous wound healing of burns and surgical wounds in rats is accelerated due to reduced oxidative stress. However, very few studies are available for the use of AuNPs in angiogenesis regulation during wound healing processes. Therefore, in this study, we will investigate the roles of AuNPs and their cooperative effect in the angiogenesis mechanism. The data obtained will contribute to our understanding concerning the possible roadmap and the control of these cues for optimal wound therapy.

肆、研究材料及研究方法

研究材料

1. Preparation of Alginate/AuNPs nanoparticles

The AuNPs will be synthesized with adaptions of methods described by Dr. Cheng-An J. Lin et al. [38]. 100 mM of DDAB or decanoic acid in toluene will be prepared as a stock solution. 25 mM of gold (III) chloride (AuCl3) in DDAB stock solution will be prepared as a gold precursor solution. 1 ml of freshly prepared TBAB solution (100 mM in DDAB stock solution) will be then added into the vigorously stirred decanoic acid solution (0.625 ml). Next, 0.8 ml of the gold precursor solution will be immediately added and a dark red solution of 6 nm gold nanoparticles will be obtained. The gold precursor solution will be then added drop-wise into the asprepared 6 nm gold nanoparticles until the color changed to a yellowish hue, which signifies the formation of 3 nm DDAB-stabilized gold nanoclusters (AuNPs@DDAB). AuNPs@DDAB will be then added to reduced lipoic acid of which the premixing molar ratio of lipoic acid to TBAB (50 mM) is 4 to 1 to produce sufficient DHLA for ligand exchange. The resulting solution will be exposed to 365 nm UV-light for 20-30 min and agglomerates of gold nanoclusters will be then obtained by ligand-exchange. After discarding the supernatants, the agglomerates will be redissolved in methanol. All solvents will be then evaporated under reduced pressure on a rotary evaporator (Laborota 4000, Heidolph) and then re-dissolved in sodium borate buffer (SBB, pH 9). Further, AuNPs@DHLA will be purified by passing it through the membrane of a 100 kDa MWCO centrifugal filter (Millipore) to remove unwanted particles, followed by the collection of using another 30 kDa MWCO centrifugal filter. 6 The purified AuNPs@DHLA will be adjusted to 40 μM for testing. It is assumed that the extinction coefficient of AuNPs@DHLA is 297000 M-1cm-1 at 420 nm. For Alginate/AuNPs nanoparticles combination, sodium alginate (Ferak, Berlin, Germany) will be first adjusted to a 5% (w/w) transparent solution using distilled water. Further, a certain amount of AuNPs solution (AuNPs@DHLA) will be added drop-wise into 5 ml of sodium alginate solution and the reaction mixture will be subsequently heated to facilitate the reduction of gold ions.

2. Characterization of Alginate/AuNPs nanoparticles

Alginate/AuNPs nanoparticles will be characterized by UV-vis spectra (Shimadzu UV3150) and transmission electron microscopy (TEM). For TEM analysis, 10 µl exosomes will be fixed with 2.5% glutaraldehyde for 2 h and will be added to a 200

mesh Formvar stabilized with carbon. The grids will be then stained with 2% uranyl acetate for 1 h. Samples will be examined with a TEM Jeol JEM-1200 EXII (Jeol, Tokyo, Japan) at 100 kV. A Zetasizer Nano-ZS DLS system (Malvern, Montréal, QC, Canada) will be used to assess the particle diameter of isolated samples. Briefly, 100 µl of each sample will be loaded into an ultraviolet microcuvette (BRAND; Essex, CT, USA) at 4 °C. The Brownian motion of each particle will be measured by the fluctuations of scattered light intensity at a wavelength of 633 nm and a fixed angle of 173°. Data points from each replicate represent an average of three automatic measurements of 12–18 runs. The average particle diameter will be obtained from the peak of the Gaussian model fit to the particle distribution and presented by PDI.

研究方法

1. HUVEC induced by CoCl₂

The HUVEC pretreated CoCl₂ will be seeded in 24 well dishes. AuNP will be also added to the culture medium. After cell-attached (about 2-4 hours), the photo will be taken every 4-8 hours for observing and comparing endothelial cell tube formation progressions.

2. MTT assay for cell viability

3-(4,5-Di-2-yl)-2,5-ditetrazolium bromide (MTT) assay was performed to evaluate the cytotoxic effect of ruscogenin. The cells were seeded in 96-well plates (3×10^3 cells/well), cultured for 24 h and treated with ruscogenin ($0.001-100~\mu M$). At the end of the incubation period, the cells were incubated with 1 mg/ml MTT solution. Three hours later, the absorbance was measured at 450 nm and the data were assessed using an ELX-800 spectrometer reader (Bio-Tek Instruments).

3. ROS assay

(DAF-FMDA:4-amino-5-methylamino-2',7'-dichlorofluorescein diacetate) The HUVEC will be seeded in a black 96-well plate. ALA will be added for 1 day. CellROX Green Reagent used in this experiment is for measuring the intracellular ROS. To measure the ROS, firstly the cells will be washed with PBS three times. Then, it will be incubated at 37 °C in a medium composed of 5 μM CellROX reagent for 30 min. The cells will be later cleaned with PBS three times and fixed with 3.7% formaldehyde for 15 min. Furthermore, a fluorescence microplate reader used here is to analyze the fluorescence by using SpextraMax M3 with the excitation set at 485 nm and the emission at 520 nm.

4. RT-PCR

Total RNA will be extracted from cultures using AllPrep DNA/RNA Mini Kit (Qiagen, Hilden, Germany) according to the manufacturer's instructions. The total RNA (500 ng) will be reverse-transcribed using the Prime Script TM RT Master Mix (TaKaRa, Japan) with a PCR System 9700 thermal cycler (GeneAmp, ABi, Carlsbad, CA, USA), and the relative levels of the indicated genes will be assessed by real-time PCR using SYBR Premix Ex Taq TM (TaKaRa, Japan) with a CFX96TM real-time system instrument (Bio-Rad, Hercules, CA, USA), according to the manufacturer's protocol. The examined genes will be angiogenic HIF-1 and VEGF.

5. Rat burn model

All animal procedures will be registered to the Animal Research Committee at National Defense Medical Center and experiments will be carried out in accordance with the approved guidelines. A total number of 40 female Sprague-Dawley rats (eight weeks of age; 220–250 g) will be purchased from Bio-LASCO Co. Ltd (Taipei, Taiwan). The method for establishing a third degree burn injury in rat will be performed according to previous study [39]. Briefly, the rats will be anesthetized with pentobarbital (50 mg/kg) intraperitoneally and separated into 2 groups: rat with treatment and rat without treatment (control). Burn injury will be then induced by immersing the dorsal part of the right hind paw into a hot water bath (85 °C) for 12 s, limit to an area of approximately 0.75 cm2 using a holed plastic template. Sham injury will be produced by immersing the dorsal part of the right hind paw into a warm water bath (35 °C) for 12 s. Alginate/AuNPs treatment will be applied twice daily to the injured surface until the scar tissue is fully formed. Rats will have free access to laboratory chow and tap water and will be kept in an experimental room whose temperature will be maintained between 21 °C and 24 °C. Rats will be euthanized after treatment periods with lethal doses of CO2 inhalation.

6. Histological analysis

After euthanasia, the burn skin tissue will be excised and fixed in a 10 % a neutral buffered formalin embedded in paraffin, and then sliced into 4-µm sections. The sections will be stained with Hematoxylin and Eosin following the manufacturer's instructions and conventional methods. The staining images will be observed using Image-Pro Plus software.

7. Immunofluorescence

The lumbar spinal cord (L4 and L5) segments will be harvested, post-fixed for 4 h, and cryoprotected in 30% 0.1 M PB buffered sucrose. A transverse section of a 25um thickness will be performed. Sections will be then rinsed in 0.01 M PBS for 10 min×3 and mounted onto slides. The sections will be blocked for 30 min in PBS containing 1% BSA, 5% donkey serum, and 0.3% Triton X-100. After removing the blocking buffer, sections will be incubated with a primary antibody against iNOS, Akt1, Akt2, Akt/protein kinase B, TrkA, and p75NTR (all antibody 1:500 dilution; all from Abcam, USA) for overnight at 4 °C. After rinsing in PBS, corresponding second antibodies (1:800; FITC conjugated donkey anti-rabbit or donkey anti-mouse IgG) will be introduced for 30 min at room temperature. The sections will be then again rinsed with PBS (10 min×3) and covered. Sections will be then photographed using an inverted fluorescent microscope (Axio Lab.A1; Carl Zeiss AG, Oberkochen, Germany) equipped with a camera (Zeiss AxioCam ICm1; Carl Zeiss AG, Oberkochen, Germany). Semiquantitative measurements of positive staining will be conducted using the ImageJ software. Controls will be made by neglecting primary antibodies followed by the same incubation procedure as described above.

8. Statistical analyses

All experiments were performed using at least three technical replicates. Statistical analyses were performed using SPSS 14.0. Data were analyzed using the Duncan test with p-values less than 0.05 considered statistically significant.

伍、研究結果

AuNPs-alginate treatment significantly increased HUVEC cell survival ratio

The hypoxia state in the lesion group significantly reduced HUVEC cell survival compared to the control group, and both AuNPs and AuNPs-alginate treatment significantly increased cell survival compared to the lesion group. Moreover, AuNPs-alginate treatment demonstrated significantly better HUVEC cell survival than AuNPs treatment. In addition, cell survival was increased as AuNPs or AuNPs-alginate doses progressed, implying the ability of AuNPs to enhance cell survival under a hypoxic environment.

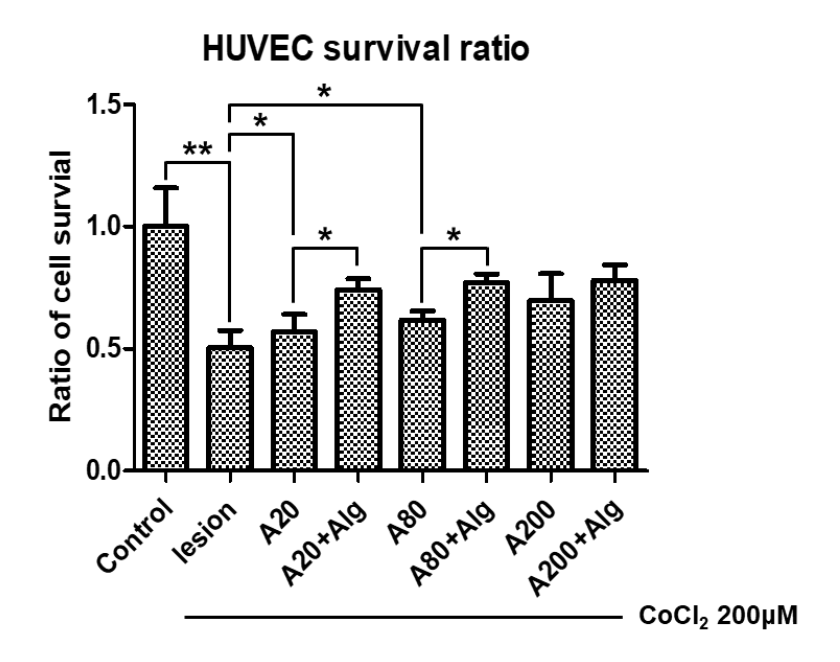


Figure 1. The ratio of HUVEC cell survival under hypoxia state affected by treatments. (*p<0.05, **p<0.01)

2. AuNPs-alginate treatment significantly reduced HUVEC cell microenvironment ROS

In compare with the lesion group, the ROS ratio of the control group was significantly lower. The ROS ratio in the AuNPs and AuNPs-alginate treated groups were also significantly lower than the lesion group. A significant outcome were shown between the AuNPs and the AuNPs-alginate treated groups with same AuNPs concentration, indicated that AuNPs-alginate treatment demonstrated significantly lower ROS in the cell microenvironment than AuNPs treatment. This result have imply that AuNPs-alginate have better antioxidant capacity than AuNPs only.

Figure 2. ROS ratio results of HUVEC cell using different concentrations of AuNPs and AuNPs + alg. (*p<0.05, **p<0.01)

3. The levels of H1F-1a and CD31 in HUVEC cells affected by treatments

Compared to the control group, the level of H1F-1 α in HUVEC cells in the lesion group was significantly higher (Figure 3). Overall, this level was reduced after AuNPs and AuNPs-alginate treatments, which was likely similar to the control group. A significant outcome was shown by AuNPs-alginate treatment. H1F-1 α , one of the important hypoxia regulation factors, accumulates under a hypoxic environment, which is caused by increasing oxidative pressure. Hence, the combination of AuNPs-alginate treatment was effective in reducing the hypoxic suppression of H1F-1 α , and therefore, lessening the oxidative stress in the cell microenvironment.

In line, the level of CD31 in HUVEC cells in the lesion group was significantly higher compared to the control group (Figure 3). Overall, this level was reduced after AuNPs and AuNPs-alginate treatments, which was likely similar to the control group. A significant outcome was shown by AuNPs-alginate treatment. CD31 is expressed on the surface of endothelial cells. The decreased level of CD31, a well-defined marker of angiogenesis, suggests the development of endothelial-to-mesenchymal cell transition, which is a key player in the remodeling of injured vessels. Hence, the combination of AuNPs-alginate treatment was effective in reducing the hypoxic suppression of CD31, and therefore, may lessen bedsores caused by wounds.

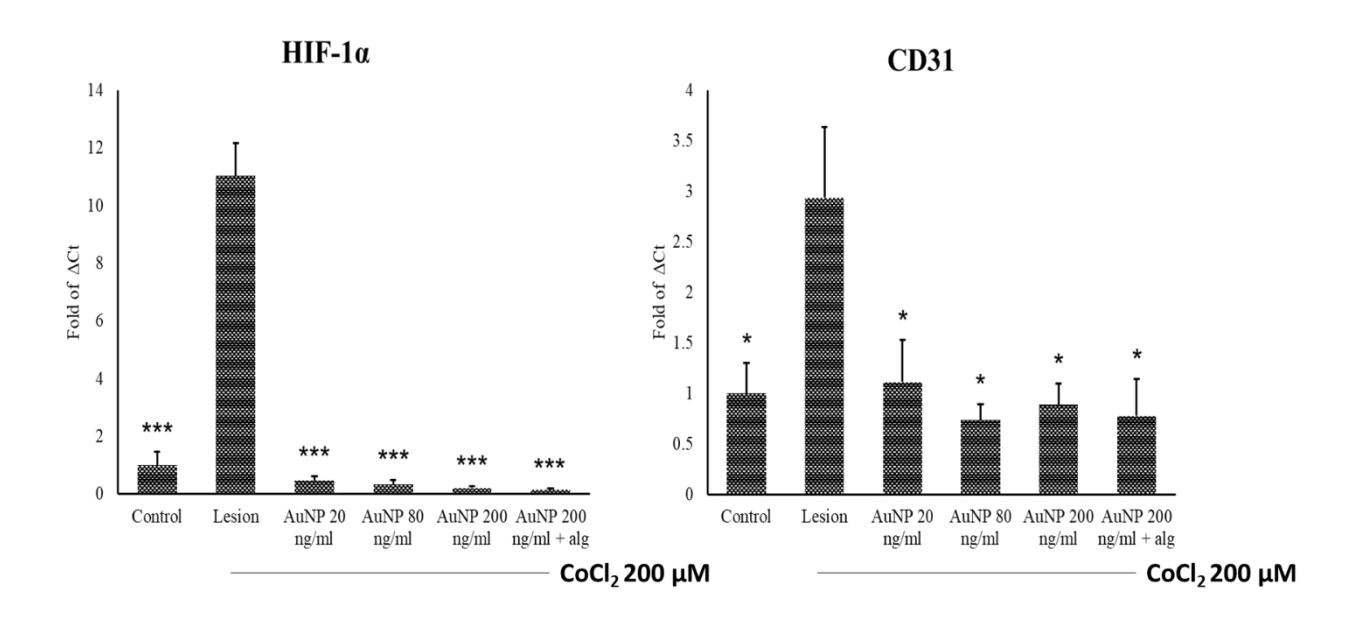


Figure 3. qPCR results of H1F-1 α and CD31 in HUVEC cell using different concentrations of AuNPs and AuNPs + alg. (*p<0.05, **p<0.01, ***p<0.001)

4. Histological Analysis of Au@Alginate Nanoparticle Polymer for Burn Wound Healing Under Different Treatment Conditions.

In this study, we investigated the effects of different treatments on burn wound healing using histological analysis. In the control group (Lesion and with no treatment) (Figure 4A), extensive epidermal damage and significant infiltration of inflammatory cells were observed. In the alginate-treated group (Figure 4B), the epidermal layer appeared more intact and decreased inflammatory cell infiltration, suggesting partial relief from the inflammatory response. The Alginate/AuNPs (20 nM) group (Figure 4C) exhibited a more complete epidermal structure. Inflammatory cells were reduced, indicating enhanced tissue repair. The Alginate/AuNPs (60 nM) group (Figure 4D) demonstrated nearly complete epidermal restoration and collagen fibers that were densely packed and well-organized, resembling healthy tissue architecture. These findings highlight the effect of AuNPs on promoting wound healing through reducing inflammation and improving collagen deposition.

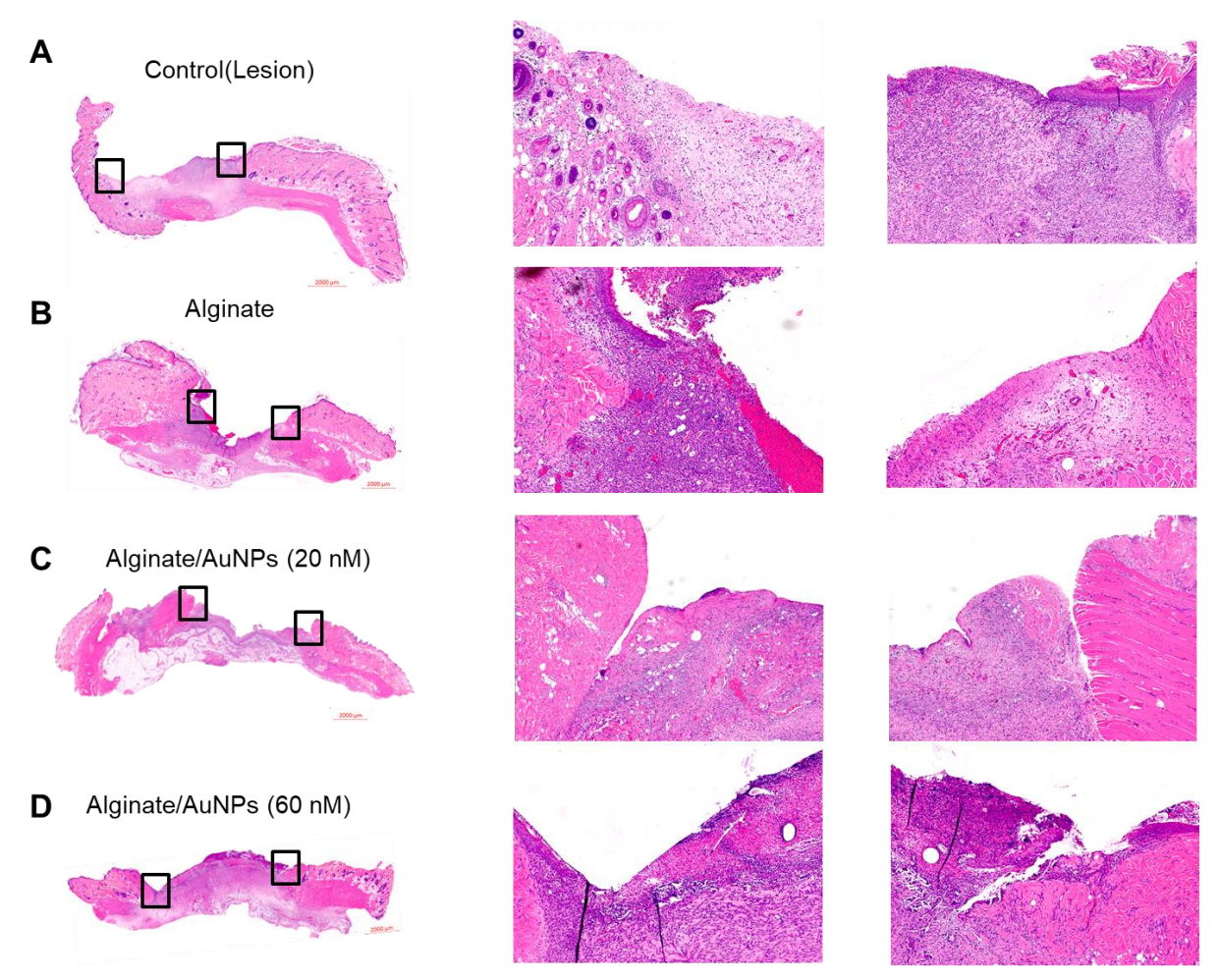


Figure 4. Histological analysis of burn wound healing under different treatments using H&E staining.

Representative histological images of burned skin sections from different treatment groups are presented: (A) Control (Lesion) group (untreated), (B) alginate-treated group, (C) Alginate/AuNPs (20 nM)-treated group, and (D) Alginate/AuNPs (60 nM)-treated group. Low-magnification images (left panels) and their corresponding high-magnification images (right panels) illustrate variations in tissue morphology across the groups.

Evaluation Following Au@Alginate Nanoparticle Polymer for Burn Wound Healing Under Different Treatment Conditions.

In this study, immunohistochemical analysis of the skin, showing stained images for various inflammatory markers were evaluated the expression of IL-1 β (Figure 5), IL-10 (Figure 6), and TNF- α (Figure 7), across four treatment groups: Control (Lesion), Alginate, Alginate/AuNPs (20 nM), and Alginate/AuNPs (60 nM). Immunohistochemistry (IHC) was performed to visualize the expression and localization of antibodies in tissue sections, with DAPI used for nuclear counterstaining.

The expression of IL-1 β and TNF- α progressively decreased across the experimental groups. IL-1 β and TNF- α are integral to the inflammatory process, acting both independently and in concert to regulate immune responses. This suggests that alginate and alginate/AuNPs treatments may contribute to an anti-inflammatory effect (Figure 5, 6). However, the decrease in IL-10 raises questions about the overall balance of inflammatory and anti-inflammatory responses that warrant further investigation (Figure 7).

Overall, the IHC staining results revealed that the use of alginate and alginate combined with AuNPs (20 nM and 60 nM) had a significant impact on the expression of key markers. Specifically, the treatments promoted the activation of RelA/NF-kB and NGFR, which are associated with cell survival and neural activity. Simultaneously, the treatments reduced the expression of pro-inflammatory markers IL-1 β and TNF- α , suggesting potential therapeutic benefits in controlling inflammation.

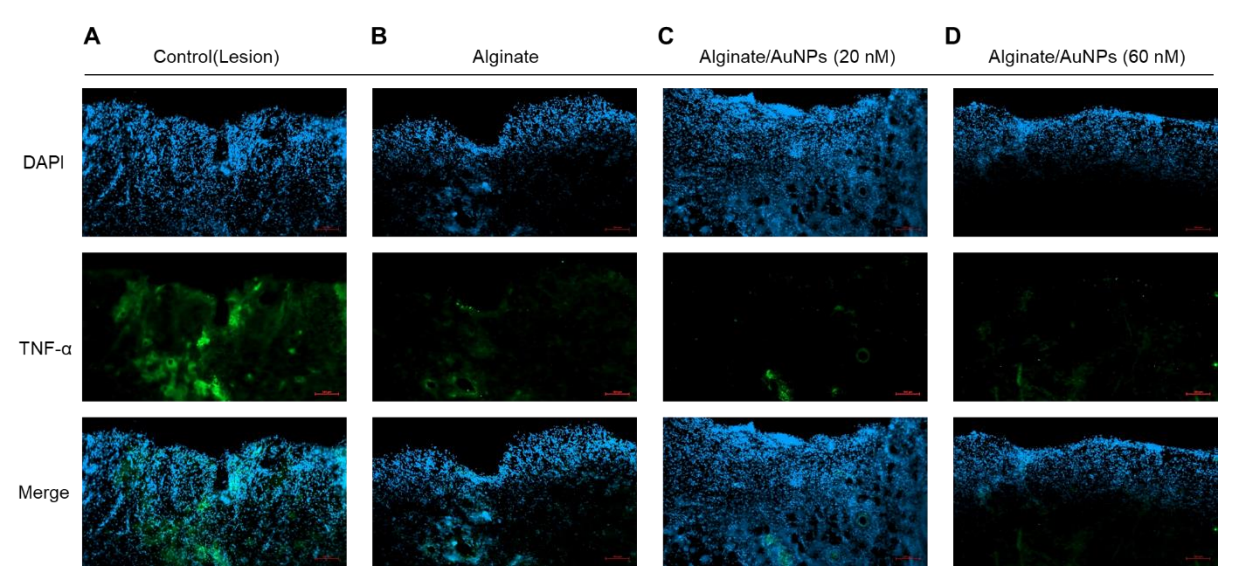


Figure 5. Immunofluorescence analysis of TNF- α in tissue sections from different treatment groups.

TNF α is a pro-inflammatory cytokine involved in inflammation, tissue damage, and healing modulation. Immunofluorescence staining showing TNF- α (antibody) in green, counterstained with DAPI (blue) to visualize cell nuclei. (A) Control (Lesion) group (untreated), (B) Alginate group, (C) Alginate/AuNPs (20 nM) group, and (D) Alginate/AuNPs (60 nM) group. Merge images show the overlap of antibody and DAPI staining for co-localization analysis.

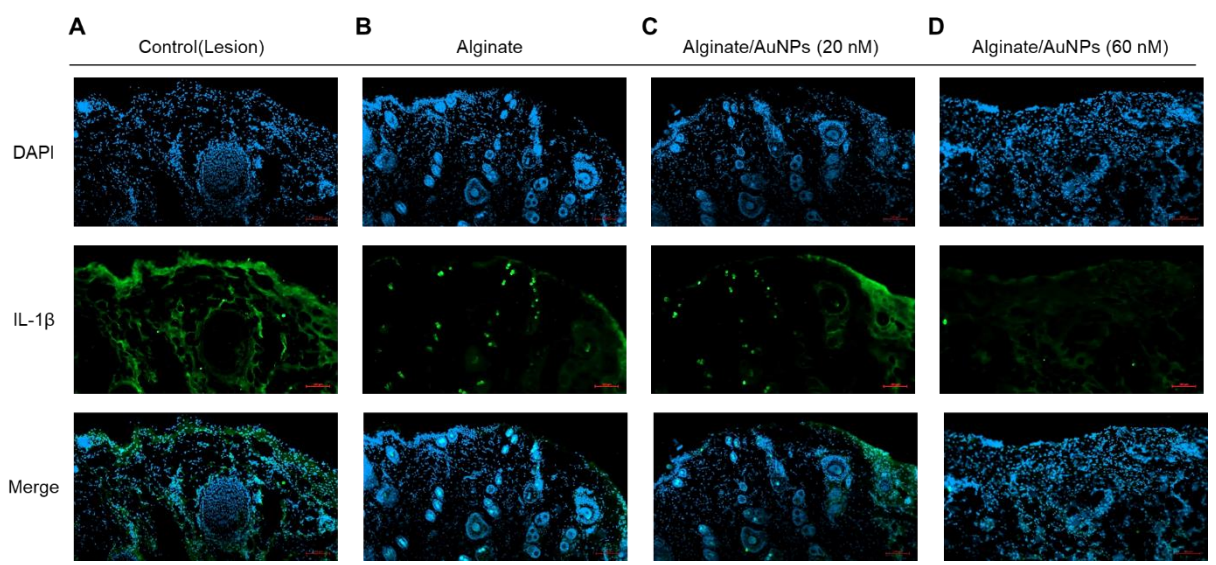


Figure 6. Immunofluorescence analysis of IL-1 β in tissue sections from different treatment groups.

IL-1β is rapidly released from damaged cells and infiltrating immune cells as a key pro-inflammatory mediator. Immunofluorescence staining showing IL-1β (antibody) in green, counterstained with DAPI (blue) to visualize cell nuclei. (A) Control (Lesion) group (untreated), (B) Alginate group, (C) Alginate/AuNPs (20 nM) group, and (D) Alginate/AuNPs (60 nM) group. Merge images show the overlap of antibody and DAPI staining for co-localization analysis.

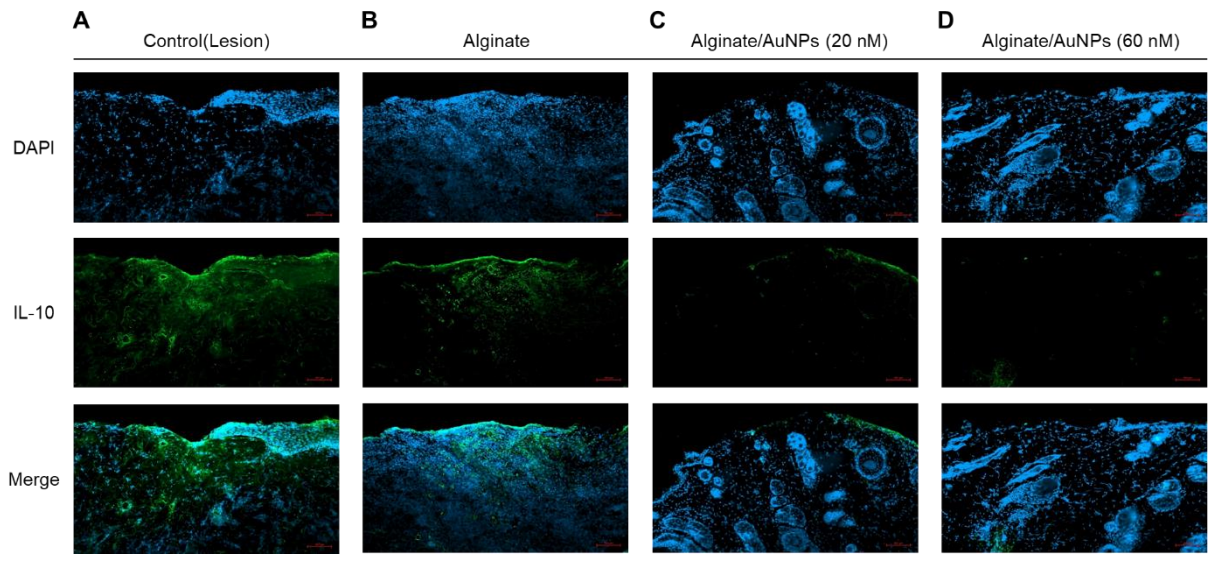


Figure 7. Immunofluorescence analysis of IL-10 in tissue sections from different treatment groups.

IL-10, which is an anti-inflammatory cytokine playing a crucial role in preventing inflammatory. Immunofluorescence staining showing IL-10 (antibody) in green, counterstained with DAPI (blue) to visualize cell nuclei. (A) Control (Lesion) group (untreated), (B) Alginate group, (C) Alginate/AuNPs (20 nM) group, and (D)

Alginate/AuNPs (60~nM) group. Merge images show the overlap of antibody and DAPI staining for co-localization analysis.

陸、結論與建議

陸 1.結論

In summary, the in vitro analyses demonstrated that AuNPs-combined alginate treatment significantly enhances cell survival, reduces ROS levels, and mitigates the hypoxic suppression of HIF-1 α and CD31, thereby potentially alleviating oxidative stress associated with wounds. This research investigated the effects of alginate/gold nanoparticles (Au@alginate) on burn wound-related neuropathy in rats. Burn wounds were induced and followed by a comprehensive analysis, including histological examination (H&E staining) and qPCR to assess the expression of inflammatory markers (IL-1 β , IL-6, and TNF- α) and nerve-related growth factor receptors. Immunofluorescence (IF) was employed to evaluate neural and skin-related markers. Our results demonstrate that AuNPs promote wound healing by reducing inflammation and enhancing collagen deposition.

陸 2.建議

The results of our study demonstrate that the AuNPs-Alginate dressing is beneficial for wound repair. A broader analysis including additional inflammation-related cytokines and neural markers could provide a more comprehensive understanding of the treatment's effects. Further investigations are necessary to assess its clinical applicability and evaluate long-term therapeutic outcomes. Future in vivo experiments will be conducted to enhance the robustness of the research findings. If our subsequent studies confirm that the AuNPs-Alginate dressing improves the wound repair process, it could be considered for treating burn-injured patients and may represent a novel strategy for the treatment and care of burn wounds.

柒、参考文獻

- 1. Fife CE, Carter MJ. Wound Care Outcomes and Associated Cost Among Patients Treated in US Outpatient Wound Centers: Data From the US Wound Registry. Wounds 24: 10–17, 2012.
- 2. Leavitt T, Hu MS, Marshall CD, Barnes LA, Lorenz HP, Longaker MT. Scarless wound healing: finding the right cells and signals. Cell Tissue Res 365: 483–493, 2016.
- 3. P. Carmeliet and R. K. Jain, Angiogenesis in cancer and other diseases, Nature, 2000, 10 407, 249–257.
- 4. R. R. Chen, E. A. Silva, W. W. Yuen and D. J. Mooney, Spatio-temporal VEGF and PDGF delivery pattern blood vessel formation and maturation, Pharm. Res., 2007, 24(2), 258–264. 3 T. P.
- 5. Richardson, M. C. Peters, A. B. Ennett, and D. J. Mooney, Polymeric system for dual growth factor delivery, Nat. Biotechnol., 2001, 19(11), 1029–1034.
- 6. M. P. Rodero and K. Khosrotehrani, Skin wound healing modulation by macrophages, Int. J. Clin. Exp. Pathol., 2010, 3(7), 643–653. 5 R. Sridharan, A. R.
- 7. Cameron, D. J. Kelly, C. J. Kearney and F. J. O'Brien, Biomaterial based modulation of macrophage polarization: A review and suggested design principles, Mater. Today, 2015, 18(6), 313–325.
- 8. J. B. Rice, U. Desai, A. K. G. Cummings, H. G. Birnbaum, M. Skornicki and N. B. Parsons, Burden of diabetic foot ulcers for medicare and private insurers, Diabetes Care, 2014, 37(3), 651–658.
- 9. Melanie Rodrigues, Nina Kosaric, Clark A. Bonham, and Geoffrey C. Gurtner. WOUND HEALING: A CELLULAR PERSPECTIVE. Physiol Rev. 2019; 99: 665–7
- 10. Lansdown AB. Calcium: a potential central regulator in wound healing in the skin. Wound Repair Regen 10: 271–285, 2002.
- 11. Yukna RA, Turner DW, Robinson LJ. Variable antigenicity of lyophilized allogeneic and lyophilized xenogeneic skin in guinea pigs. J Periodontal Res 12: 197–203, 1977.
- 12. Winter GD. Formation of the scab and the rate of epithelization of superficial wounds in the skin of the young domestic pig. Nature. 1962;193:293-294.
- 13. Kim JO, Park JK, Kim JH, Jin SG, Yong CS, Li DX, Choi JY, Woo JS, Yoo BK, Lyoo WS, Kim JA, Choi HG. Development of polyvinyl alcohol-sodium alginate

- gel-matrixbased wound dressing system containing nitrofurazone. Int J Pharm. 2008;359(1-2):79-86.
- 14. Lin SY, Chen KS, Run-Chu L. Design and evaluation of drug-loaded wound dressing having thermoresponsive, adhesive, absorptive and easy peeling properties. Biomaterials. 2001;22(22):2999-3004.
- 15. Kuo CK, Ma PX. Ionically crosslinked alginate hydrogels as scaffolds for tissue engineering: part 1. Structure, gelation rate, and mechanical properties. Biomaterials. 2001;22(6):511-521.
- 16. Wiegand C, Heinze T, Hipler UC. Comparative in vitro study on cytotoxicity, antimicrobial activity, and binding capacity for pathophysiological factors in chronic wounds of alginate and silver-containing alginate. Wound Repair Regen. 2009; 17(4): 511-521.
- 17. Dumville JC, O'Meara S, Deshpande S, Speak K. Alginate dressings for healing diabetic foot ulcers. Cochrane Database Syst Rev. 2013;(6): Cd009110.
- 18. Alsharabasy AM, Moghannem SA, El-Mazny WN. Physical preparation of alginate/chitosan polyelectrolyte complexes for biomedical applications. J Biomater Appl. 2016;30(7):1071-1079.
- 19. Abdelrahman T, Newton H. Wound dressings: principles and practice. Surgery (Oxford). 2011;29(10):491-495.
- 20. Sood A, Granick MS, Tomaselli NL. Wound dressings and comparative effectiveness data. AdvWound Care (New Rochelle). 2014;3(8):511-529.
- 21. Miyazaki T, Shirakami Y, Kubota M, Ideta T, Kochi T, Sakai H, Tanaka T, Moriwaki H, Shimizu M. Sodium alginate prevents progression of non-alcoholic steatohepatitis and liver carcinogenesis in obese and diabetic mice. Oncotarget. 2016;7(9):10448-10458.
- 22. Shende P, Patel D. Potential of Tribological Properties of Metal Nanomaterials in Biomedical Applications. Adv Exp Med Biol. 2020;1237:121-134.
- 23. Mofazzal Jahromi MA, Sahandi Zangabad P, Moosavi Basri SM, Sahandi Zangabad K, Ghamarypour A, Aref AR, Karimi M, Hamblin MR. Nanomedicine and advanced technologies for burns: Preventing infection and facilitating wound healing. Adv Drug Deliv Rev. 2018;123:33-64.
- 24. Schneider M, Stracke F, Hansen S, Schaefer UF. Nanoparticles and their interactions with the dermal barrier. Dermatoendocrinol. 2009;1(4):197-206.
- 25. Bolanos K, Kogan MJ, Araya E. Capping gold nanoparticles with albumin to improve their biomedical properties. Int J Nanomedicine. 2019;14:6387-6406.
- 26. Chen SA, Chen HM, Yao YD, Hung CF, Tu CS, Liang YJ. Topical treatment with

- anti-oxidants and Au nanoparticles promote healing of diabetic wound through receptor for advance glycation end-products. Eur J Pharm Sci. 2012;47(5):875-883.
- 27. Church D, Elsayed S, Reid O, Winston B, Lindsay R. Burn wound infections. Clin Microbiol Rev. 2006;19(2):403-434.
- 28. Stoodley P, Sauer K, Davies DG, Costerton JW. Biofilms as complex differentiated communities. Annu Rev Microbiol. 2002;56:187-209.
- 29. Cucarella C, Tormo MA, Ubeda C, Trotonda MP, Monzón M, Peris C, Amorena B, Lasa I, Penadés JR. Role of biofilm-associated protein bap in the pathogenesis of bovine Staphylococcus aureus. Infect Immun. 2004;72(4):2177-2185.
- 30. N Yuan, K Shao, S Huang, C Chen. Chitosan, alginate, hyaluronic acid and other novel multifunctional hydrogel dressings for wound healing: A review. International Journal of Biological. Volume 240, 15 June 2023, 124321
- 31. A Froelich, E Jakubowska, M Wojtyłko, B Jadach. Alginate-based materials loaded with nanoparticles in wound healing. Pharmaceutics 2023, 15(4), 1142
- 32. G Mao, S Tian, Y Shi, J Yang, H Li, H Tang Preparation and evaluation of a novel alginate-arginine-zinc ion hydrogel film for skin wound healing. Carbohydrate Polymers Volume 311, 1 July 2023, 120757